

388 **Supplemental Figures**

Name	FP41 IC50 (M)	FP38 IC50 (M)	FP46 IC50 (M)	Average IC50 (M)	Mechanism
Alobresib	1.04E-07	1.404E-07	7.122E-08	<b>1.0514E-07</b>	BET inhibitor
Podofilox	6.49E-09	1.503E-08	6.562E-09	<b>9.362E-09</b>	Topoisomerase II inhibitor
Staurosporine	2.71E-07	5.194E-08	6.863E-07	<b>3.3648E-07</b>	PKC $\alpha$ , PKC $\gamma$ , PKC $\eta$ inhibitor
SKLB-23bb	8.44E-08	1.742E-05	9.481E-08	<b>5.86639E-06</b>	HDAC6 inhibitor
GSK1324726A	1.54E-07	2.475E-07	1.045E-07	<b>1.68533E-07</b>	BRD2, BRD3, BRD4 inhibitor
(S)-(+)-Camptothecin	1.17E-07	6.757E-07	2.102E-07	<b>3.342E-07</b>	Topoisomerase I inhibitor
Gemcitabine	7.69E-08	1.233E-06	1.686E-07	<b>4.92843E-07</b>	DNA synthesis inhibitor
CPI203	1.53E-07	1.604E-07	1.091E-07	<b>1.40733E-07</b>	BRD4 inhibitor
NSC228155	2.59E-06	3.216E-07	2.789E-06	<b>1.90087E-06</b>	EGFR activator
BET Bromodomain Inhibitor	3.76E-07	3.445E-07	2.477E-07	<b>3.22667E-07</b>	BET inhibitor
Panobinostat	1.43E-08	3.575E-08	2.768E-08	<b>2.58967E-08</b>	HDAC inhibitor
Quisinostat	9.12E-09	1.162E-08	1.983E-08	<b>1.35243E-08</b>	HDAC inhibitor
Fimepinostat	5.96E-09	1.758E-08	9.285E-09	<b>1.09427E-08</b>	HDAC and PI3K inhibitor
Cucurbitacin B	4.84E-08	1.41E-08	5.111E-08	<b>3.78567E-08</b>	PI3K/AKT inhibitor
Romidepsin	3.16E-14	8.916E-10	1.269E-09	<b>7.20211E-10</b>	Class I HDAC inhibitor
AZD5153	9.04E-08	8.867E-08	6.833E-08	<b>8.24767E-08</b>	BRD4 inhibitor
Mivebresib	9.96E-08	1.877E-07	8.921E-08	<b>1.2549E-07</b>	BET inhibitor
ABBV-744	8.127	2834	0.05655	<b>947.3945167</b>	BRD4 inhibitor
Quisinostat 2HCl	5.42E-09	6.754E-09	1.385E-08	<b>8.674E-09</b>	HDAC inhibitor
666-15	5.89E-05	0.0005853	0.002194	<b>0.00094607</b>	EGFR inhibitor
Velcade	4.34E-09	1.487E-08	3.519E-09	<b>7.57633E-09</b>	Proteasome inhibitor

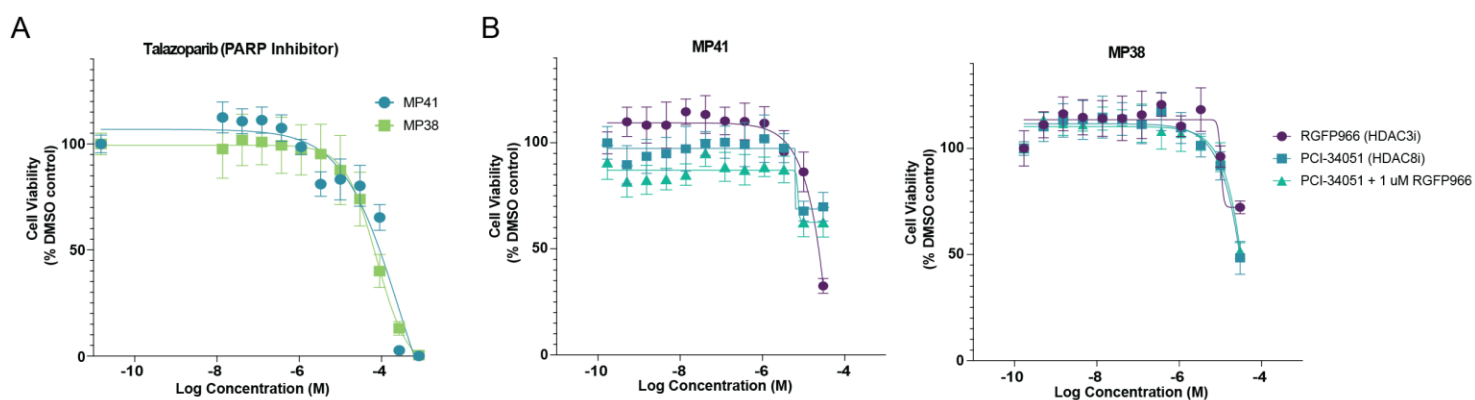
389

390 **Supplemental Table 1. Primary screen results.** IC<sub>50</sub> (M) values of the hit compounds identified by the primary screen for  
 391 each UM cell line, along with the mechanism of action of each compound.

392

393

394



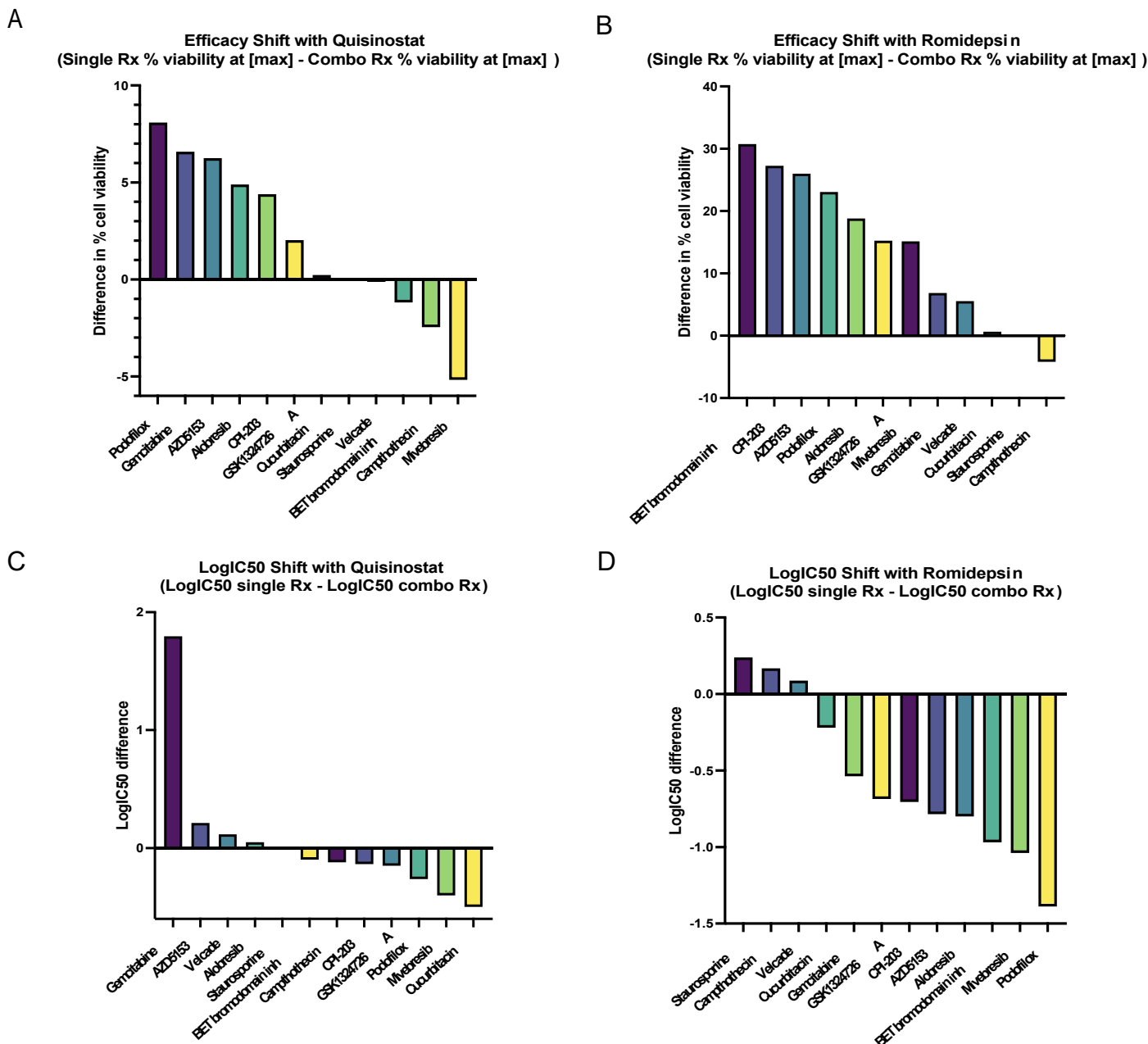
395

396

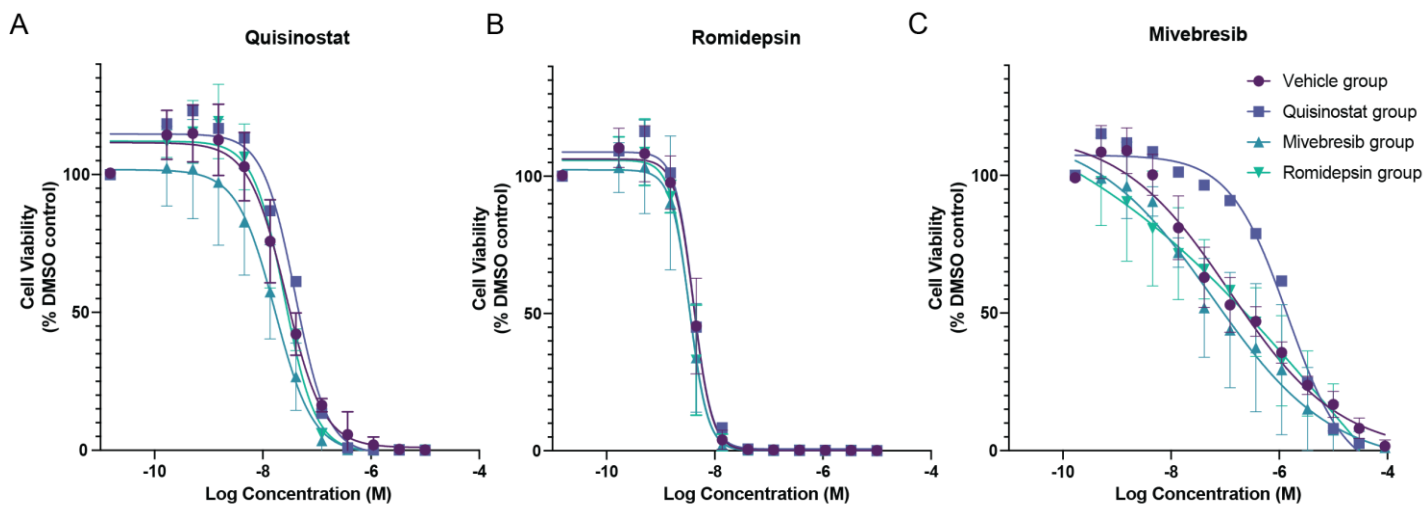
397

398

**Supplemental Figure 1. PARP inhibitor, HDAC3 inhibitor, and HDAC8 inhibitor concentration-response testing. (A)** Concentration-response curves of MP41 and MP38 cells treated with the PARP inhibitor talazoparib. **(B)** Concentration-response curves of MP41 and MP38 cells treated with HDAC3 and HDAC8 inhibitors. N = 4 for each concentration.



**Supplemental Figure 2. Synergistic tests of quisinostat and romidepsin with other candidate compounds. (A)** Difference in percent cell viability at the highest concentration (10  $\mu$ M) for cells treated with quisinostat plus EC<sub>20</sub> of other candidate compound relative to cell viability when treated with only 10  $\mu$ M quisinostat. Greater positive values indicate better synergy. **(B)** Difference in percent cell viability at the highest concentration (10  $\mu$ M) for cells treated with romidepsin plus EC<sub>20</sub> of other candidate compounds relative to cell viability when treated with only 10  $\mu$ M romidepsin. Greater positive values indicate better synergy. **(C)** Log IC<sub>50</sub> shift of cells treated with Quisinostat and the EC<sub>20</sub> of other candidate compounds relative to cells treated with only quisinostat. Greater positive values indicate better synergy. **(D)** Log IC<sub>50</sub> shift of cells treated with romidepsin and the EC<sub>20</sub> of other candidate compound relative to cells treated with only romidepsin. Greater positive values indicate better synergy.



410

411

412

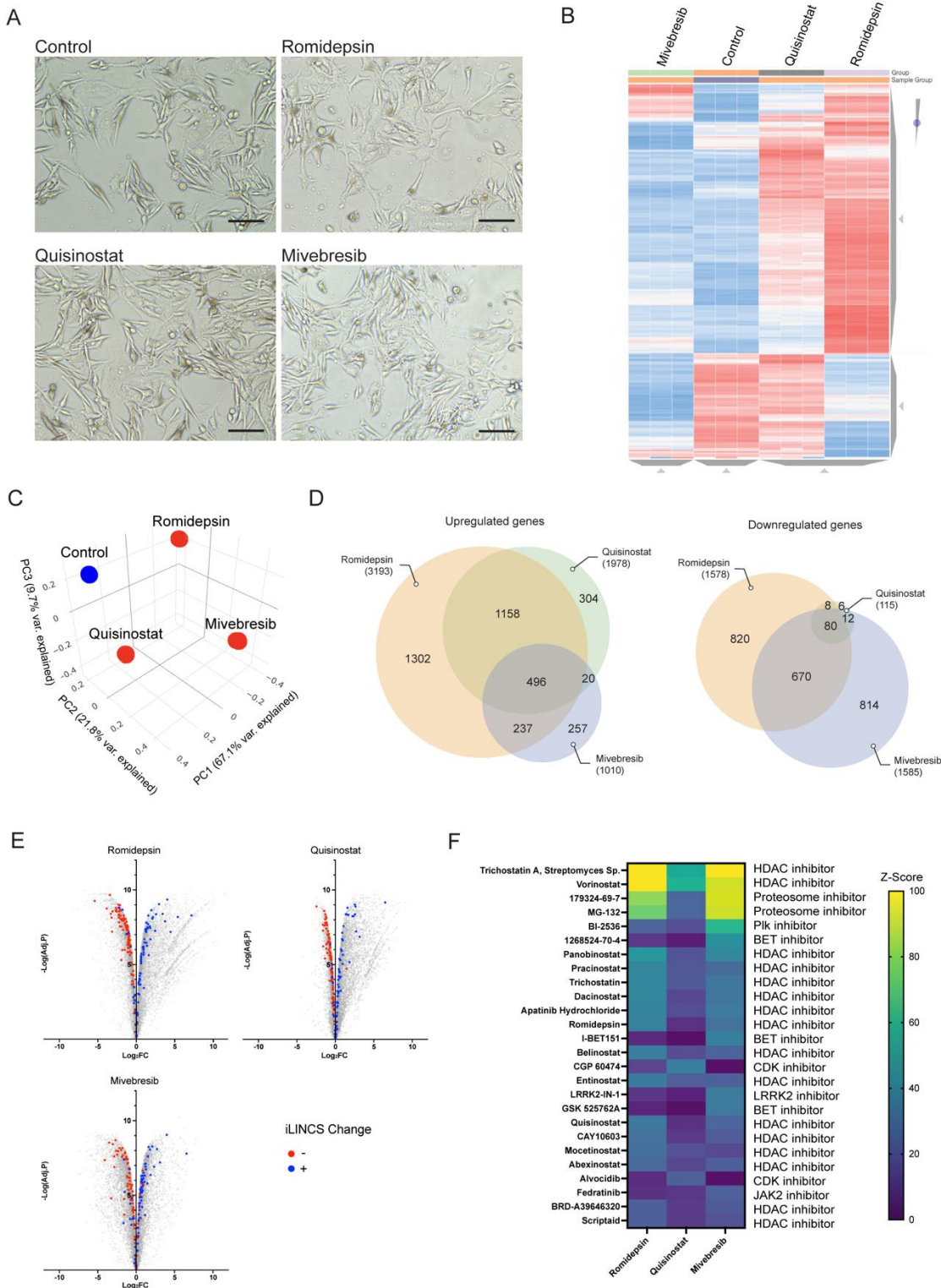
413

414

415

416

**Supplemental Figure 3. Ex vivo testing of acquired drug resistance in vehicle- and treated tumor cells from murine livers.** (A) Concentration-response curve of quisinostat treatment of MP41 cells extracted from mouse liver tumor samples averaged for each treatment group (vehicle n = 3; quisinostat n = 1, mivebresib n = 4, romidepsin n = 3). (B) Concentration-response curve of romidepsin treatment of MP41 cells extracted from mouse liver tumor samples averaged for each treatment group. (C) Concentration-response curve of mivebresib treatment of MP41 cells extracted from mouse liver tumor samples averaged for each treatment group.



417

418

419

420

421

422

423

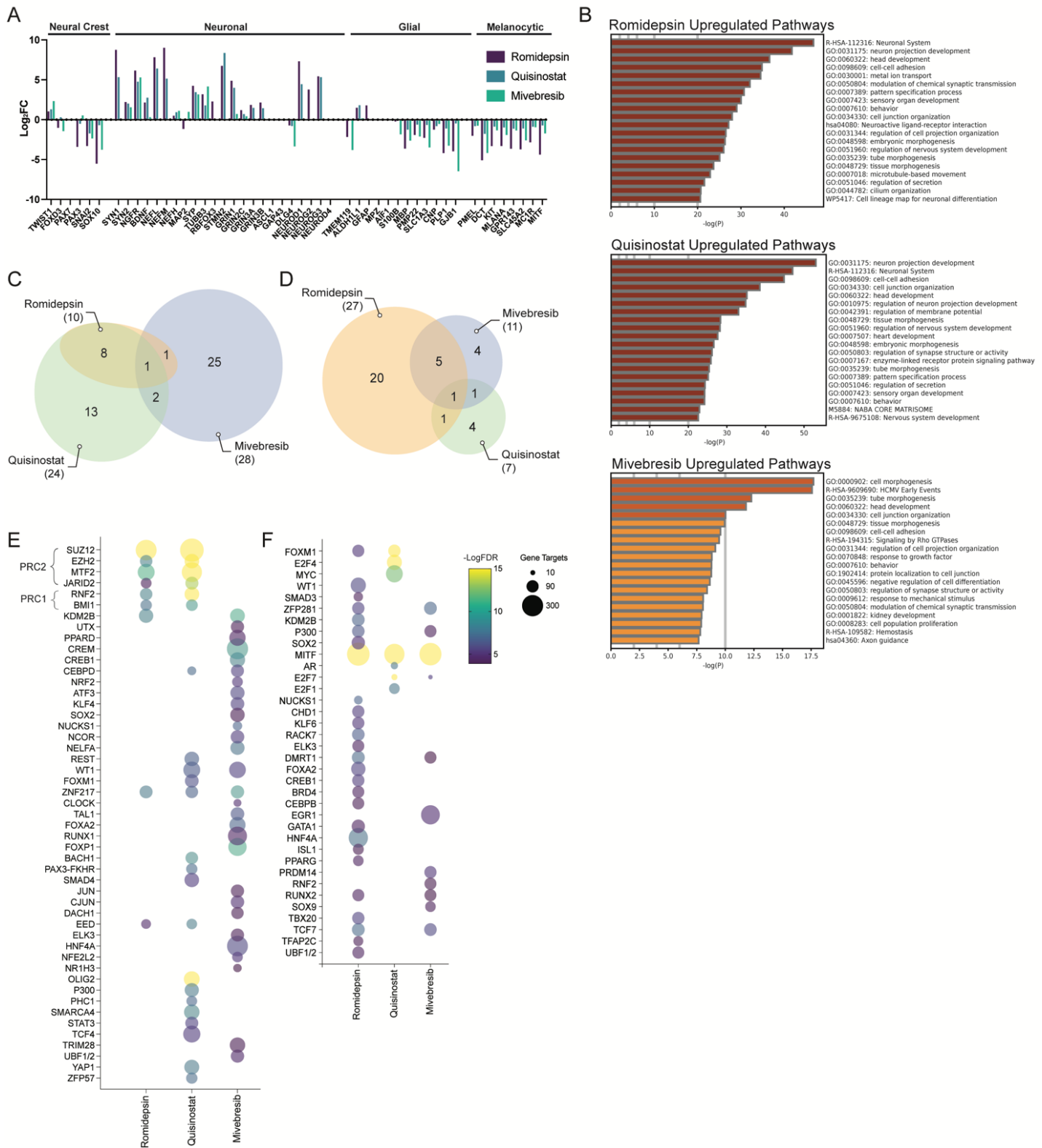
424

425

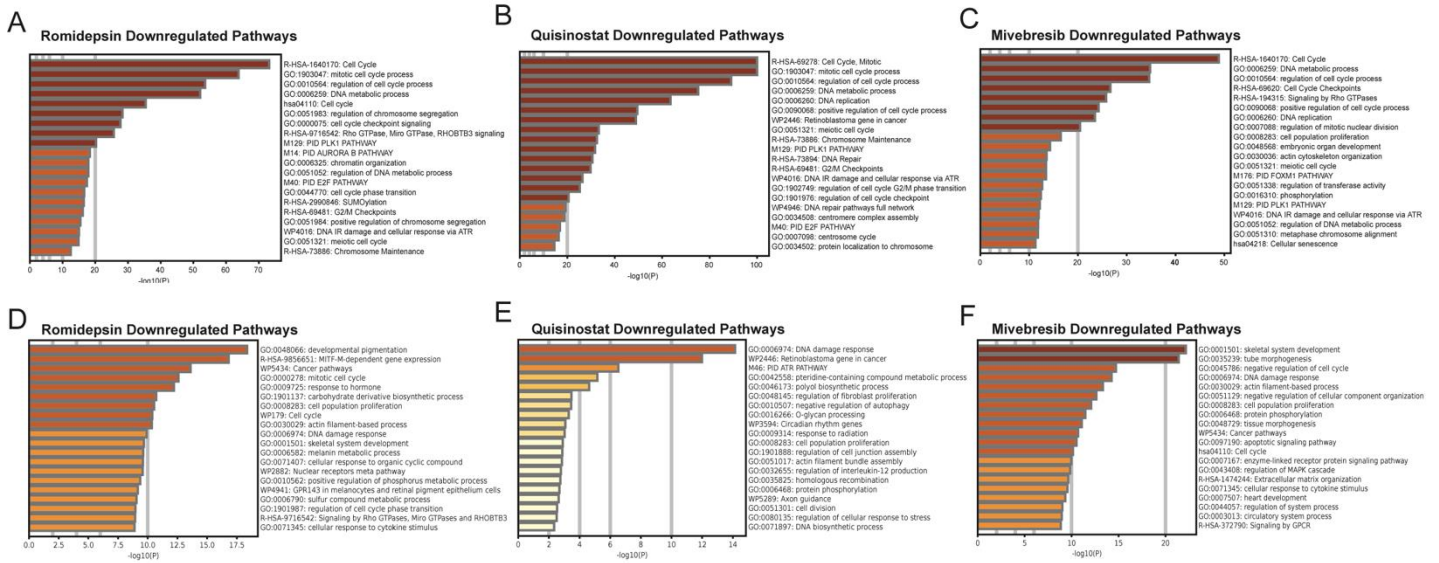
426

427

**Supplemental Figure 4. RNA-seq analysis of MP46 cells treated with candidate compounds for 24 h. (A)** Images of MP46 cells treated with each compound for 24 hours. Scale bar = 100 µm. **(B)** Heatmap clustering of changes in gene expression of MP46 cells per treatment group (n = 3 per condition). **(C)** PCA clustering of replicates for each treatment in MP46 cells. **(D)** Venn diagram depicting overlaps between the treatment groups of significantly upregulated and downregulated genes in drug-treated MP46 cells. **(E)** Volcano plot of changes in gene expression relative to the control for each treatment group in MP46 cells. Blue and red dots are 180 genes found to be consistently dysregulated as a result of eight HDAC inhibitor treatments in iLINC5. Blue dots are genes that were consistently upregulated by HDAC inhibitor treatment, while red dots are genes that were consistently downregulated. **(F)** Heatmap of perturbations inducing similar gene expression signatures to romidepsin, quisinostat, and mivebresib in MP46s using iLINC5 connected perturbation analysis.



**Supplemental Figure 5. BET and HDAC inhibition mechanisms and pathway changes in MP46 cells. (A)** Changes in the expression ( $\log_2$  FC) of genes associated with some neural-crest-derived cell identities in drug-treated MP46 cells. **(B)** Upregulated pathways in drug-treated MP46 cells predicted from list of significantly upregulated genes in each treatment group ( $\log_2$  FC > 1.5, adj. p < 0.05). **(C)** Venn diagram showing overlaps in predicted transcription factors with upregulated gene targets in MP46 cells, determined by ChIP-seq data (ChIP Enrichment Analysis (ChEA)). **(D)** Venn diagram showing overlaps in predicted transcription factors with downregulated gene targets in MP46 cells, determined by ChIP-seq data. **(E)** Bubble plot of the top predicted transcription factors with upregulated targets in MP46 cells for the tested compounds. **(F)** Bubble plot of the top predicted transcription factors with downregulated targets in MP46 cells for the tested compounds.



**Supplemental Figure 6. Pathways downregulated by each drug in MP41 and MP46 cells. (A-C)** The top 25 downregulated pathways in each treatment group were determined by Metascape analysis of the significantly downregulated genes in MP41 cells ( $\log_2$  FC < -1.5, adj. P value < 0.05). **(D-F)** The top 25 downregulated pathways in each treatment group were determined by Metascape analysis of the significantly downregulated genes in MP46 cells ( $\log_2$  FC < -1.5, adj. P value < 0.05).